Analysis of RTD Curves from a Molecular Evaporator

[a]J. CVENGROŠ, [a]M. VALKO, [a]Š. POLLÁK, and [b]J. LUTIŠAN

[a]*Department of Physical Chemistry, Faculty of Chemical Technology, Slovak University of Technology, SK-812 37 Bratislava*
e-mail: cvengros@chtf.stuba.sk

[b]*HighChem, Ltd., Jána Stanislava 35, 841 05 Bratislava*

Received 21 April 1999

In the present work the residence time distribution curves (RTD curves) for a liquid film on an evaporating cylinder are presented for a wiper with cylindrical wiping elements from PTFE having a deep screw thread of a great lead on their surface. The wiping elements bear on the evaporating cylinder due to centrifugal force and roll over it. The analysis of both RTD curves and mean residence times shows that there are three different regimes covering flow of the film over the evaporating cylinder in dependence on the process parameters, like liquid load and the peripheral speed of wiper. Attention is paid to the regime for which the RTD curves have a nonconventional elongated multipeak character with markedly longer mean residence times. A model for liquid transport over the evaporating cylinder is proposed for this regime. The passage channels of the profiled wiper element form the liquid into strands which are then moved down along the screw. Each liquid strand has its elementary distribution curve whereby the number of the elementary curves can be stated from material balance and construction parameters of the wiping element. In summary, the RTD curve is then a linear combination of these elementary distribution curves.

The wiping of a liquid film on the evaporating area of a molecular evaporator is a key operation implicating efficient, powerful, and also gentle distillation of a heat-sensitive substance without thermal hazard.

In a wiped film evaporator, the liquid in the film on the evaporating surface is continually mixed and evenly distributed over the whole evaporating cylinder. Advantageous conditions for the heat and mass transfer are thus created, thermal gradients in the film formed as a result of intense evaporation are compensated, cleaning of the evaporating surface from deposits and resinous substances is ensured, the whole evaporating surface utilization is reached, and a sufficient quantity of the liquid is ensured even in cylinder's lower parts. Favourable effects of wiping will be manifested at high evaporation rates up to 100 kg m^{-2} h^{-1} without thermal degradation, while the separation power is close to a theoretical value [1]. However, the evaporator's design remains simple. It is also possible to construct large apparatus with evaporating areas up to 40 m^2 [2]. The average thickness of the wiped film ranges from 0.1 mm to 0.5 mm depending on the viscosity, liquid load, wiper's peripheral speed, and the type of wiper. In evaporators with appropriately designed wipers, it is possible to treat liquids of a viscosity at operating temperature up to 5—10 Pa s.

Experimental results [3] as well as model study results [4, 5] show that the main resistance to mass transfer is in the liquid film on the evaporating cylinder. It is necessary that the next development of evaporators with respect to increasing their output must be aimed at the improvement of the hydrodynamic conditions on the evaporating cylinder. At present, the distillation space geometry in molecular evaporators, particularly in those of larger diameters (evaporating cylinders above 200 mm), tends to be a concave evaporating area formed on the inner side of an externally heated cylinder, and centrifugal force is utilized in order to obtain a vigorous and defined bearing of wiping elements on the evaporating surface. The wiper is made up of a massive basket construction which rotates around the evaporator's axis together with the wiping elements placed on supports at regular intervals parallel to the evaporator's axis and relatively close to the evaporating area.

Our development of a molecular evaporator wiper for a concave evaporating surface resulted in a roller wiper [6] (Fig. 1) seated on pins in locating grooves of a bearing trough. There is a deep screw thread with a great lead on the PTFE roller wiper. During the rotation of the wiping basket, the roller wiper bears on the evaporating surface due to centrifugal force. The wiper does not gather the liquid in front

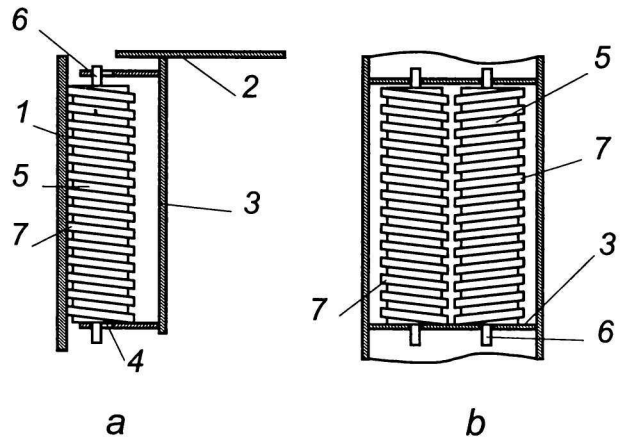

Fig. 1. Profiled-surface roller wiper, simple (*a*), twinned (*b*). *1.* Evaporating cylinder, *2.* wiping basket, *3.* bearing channel, *4.* locating groove, *5.* wiping element, *6.* pin, *7.* screw thread.

of it into a longitudinal wave, but orientates the liquid and forms it into strand-like structures, allowing it to pass through the thread openings, and causing complex intense motion. The role of the screw thread on the wiping element surface is to substantially increase the wiping element's permeability for the liquid and to minimize the longitudinal wave formation before the wiper. This should result in increased hold-up of the liquid on the evaporating surface subsequently prolonging its residence time. According to the thread lead orientation (upward or downward), the particles of a liquid attain speed components oriented either upward or downward. The liquid possibly captured by threads is returned from the bearing trough by centrifugal force onto the evaporating surface. Increased mixing of the liquid in the film can be obtained *via* a couple of closely placed roller wipers on the support, particularly if the thread lead orientations are different (Fig. 1*b*). Roller wiper peripheral speed ranges from 1 to 3 m s^{-1}.

In our preceding study, we discussed the development and testing of this new type of wiper for a molecular evaporator having a cylindrical wiping element with a deep screw thread with great lead on its surface [7]. For various peripheral liquid loads on the top of the evaporator and for various peripheral wiper speeds, residence time distribution curves (RTD curves) were measured. It was shown by an analysis of these curves that there are several regimes for the flow of liquid on the evaporating unit as a result of the wiper's action. A nontraditional and interesting flat shape of the RTD curve with several indistinct peaks observed at a certain combination of evaporator liquid load with wiper peripheral speed initiated us to study the relevant field in more considerable detail. In this paper, we publish results of this study and endeavour to make a physical interpretation of the measured relations.

EXPERIMENTAL

Evaporator and Wiper

Measurements were performed in a MO 150 molecular evaporator of our own construction. The evaporator's diameter and height are 150 mm and 600 mm, respectively.

The wiper is made up of two sets of wiping rollers on two pins relatively shifted by 180° The number of wiping rollers on one pin is five, the height of one roller is 108 mm, its diameter is 18 mm. The screw thread on its surface is clockwise with a pitch of 4 mm per a thread, the gap width is 2.5 mm, the ridge thickness is 1.5 mm and the thread depth is 2 mm. The free cross-sectional area for liquid flow is 62 %.

The wiper is driven by an electric motor at 1360 min^{-1} at 50 Hz with a reducing gear ratio 1:4, while motor revolutions can be adjusted by a frequency converter. The wiper can rotate in both directions. The measurements presented in this study were performed on a right-handed screw thread rotating from the right to the left.

Residence Time Distribution Curves

When investigating film wiping conditions, residence time distribution curves (RTD curves) of tracer concentration were used [8]. These curves were obtained from conductivity measurements after transformation into concentration functions. The conductivity sensor was made up of a ring with an oblique outer edge just under the wiper. The second electrode was the evaporator's jacket. Conductivity was measured by a conductometer linked to a PC. The computer program evaluates the mean value of ten measurements and the minimum sampling interval is 1 s.

The test liquid was a mixture of tri- and tetraethylene glycols with a dynamic viscosity of 50 mPa s at the measurement temperature (22 °C). The measurements were performed in the open evaporator without distillation. When the feed reached steady state, 1 cm^3 of a tracer (saturated solution of NaCl in water) was injected into the liquid flow in the inlet tube the outlet of which is above the plate on the top of the rotating wiper within about 0.5 s. The beginning of the measurement was derived from the logic signal from the tracer sample.

Mean residence time τ, defined as the first moment of residence time distribution around the onset, was determined from the following equation

$$\tau = \frac{\int_0^t tc(t)\mathrm{d}t}{\int_0^t c(t)\mathrm{d}t} \qquad (1)$$

Basic measurements were performed at four different wiper peripheral speeds, v, and at three different liquid loads, Γ. For each value of the specified parameters, five to six measurements were performed.

Analysis of RTD Curves

Since the experimental residence time distribution functions exhibit overlapping bands, we attempted to perform a deconvolution analysis. Such an analysis was done using a Fourier deconvolution of the resulting RTD profile into elementary curves. This technique was described for the first time by *Kirmse* and *Westenberg* [9]. These authors assumed a fixed line shape for individual bands (gaussians with constant half-width), they varied only the intensity and centre of the peak. General theory of self-deconvolution, which enables us to resolve extensively overlapping bands, was developed by *Kauppinen* [10]. The relationship between $Y(x)$ and its interferogram $I(w)$ is described by the equation

$$Y(x) = \int_{-\infty}^{+\infty} I(w) \exp(\mathrm{i}2\pi x w)\mathrm{d}w = F\{I(w)\} \quad (2)$$

where

$$I(w) = \int_{-\infty}^{+\infty} Y(x) \exp(-\mathrm{i}2\pi x w)\mathrm{d}x = F^{-1}\{Y(x)\} \quad (3)$$

$F\{\}$ represents a Fourier transformation and $F^{-1}\{\}$ represents an inverse transformation.

Any curve $Y(x)$ can be expressed as deconvolution of line shape function $G(x)$ and $Y'(x)$ according to the expression

$$Y(x) = G(x) * Y'(x) = \int_{-\infty}^{+\infty} G(x')Y'(x-x')\mathrm{d}x' \quad (4)$$

Applying a Fourier transform on both sides of eqn (4) we obtain an interferogram corresponding to a deconvolution RTD curve.

Deconvolution is the simplest, when we know the analytical expression for the shape of each band of resulting curve. This is only possible when we know a physical meaning determining the shape of each band. However, very often (including also spectral problems), we do not know a physical origin determining the shape of the bands. In such cases it is possible to use approximative functions without additional physical characterization. This method we have applied to our experimental RTD curves.

RESULTS AND DISCUSSION

As mentioned at the beginning, an unusual RTD curve shape was found at certain wiper peripheral speeds at a given evaporator liquid load and viscosity when studying properties of the developed wiper. This is shown in Fig. 2 which is composed of our measurements published in [7]. At a low wiper peripheral speed below 0.6 m s^{-1}, the relevant RTD curve (curve *1* in Fig. 2) has the Gaussian shape with a relatively broad peak and elongated descending part. Curve *2* in Fig. 2 measured at a higher peripheral speed, has a completely different multipeak character without maxima. When further increasing the wiper peripheral speed above 2 m s^{-1}, RTD curves revert to a Gaussian shape again (curves *3* and *4*).

The analysis of RTD curves at various wiper's frequencies shows that there are three different hydraulic regimes in the wiped film on the evaporating cylinder.

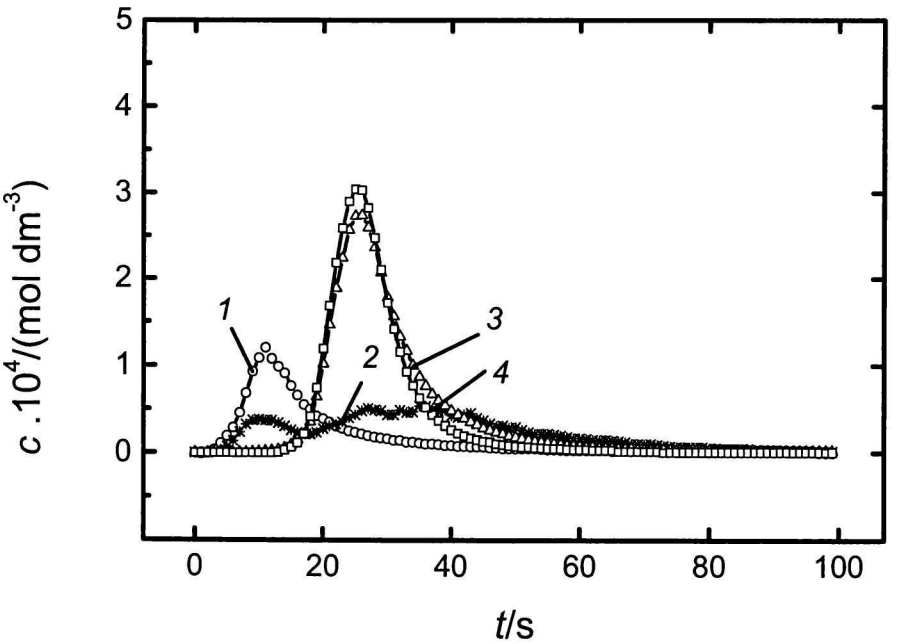

Fig. 2. Residence time distribution curves for wiped film at different wiper peripheral speeds. $\Gamma = 4.0$ dm^3 dm^{-1} h^{-1}, $\mu = 50$ mPa s. *1.* $v = 0.64$ m s^{-1}; *2.* $v = 1.14$ m s^{-1}; *3.* $v = 1.92$ m s^{-1}; *4.* $v = 2.68$ m s^{-1}.

For the first low peripheral speed regime, an RTD curve is characterized by one, not very marked peak with an extended tail. For the wiper studied and a test liquid with a viscosity of 50 mPa s, this process is observed at peripheral speeds up to about 0.6 m s^{-1} at a liquid load of 4 dm^3 dm^{-1} h^{-1}. The profiled-surface wiping element, which bears on the evaporator due to the effect of centrifugal force, directs the liquid to pass through its passage channels thus forming it into strands having increased thickness. The liquid strands disappear relatively shortly after the wiping element has passed because of surface tension effects, and a continuous, more or less undulated laminar liquid film flowing downward is created.

The character of wiping changes with the peripheral speed. There is a certain interval of peripheral speeds where, at a given liquid load, liquid viscosity, and wiper design, the liquid moves on the evaporation cylinder mostly in the form of liquid strands. These strands, which tend to deflect downward after leaving the passage channels, do not have sufficient time to level, merge, and disappear, and they are captured at a lower level in the passage channels of the subsequent wiping element. Small portions of the liquid from a higher strand flow to a lower one, but the major part of the liquid makes an intricate movement in the strands downward along the screw thread. This is manifested by an increase of the liquid residence time and by an increase of liquid hold-up on the evaporating cylinder. In this regime, the RTD curve loses its typical shape, changing it to an elongated one with several small peaks. This corresponds to a gradual output of the tracer at the screw thread end at the bottom of the evaporator. The mean residence time is longer at the beginning of the strand regime than at its end. Under the measurement conditions (wiper of the design described above, liquid load of 4 dm^3 dm^{-1} h^{-1}, and viscosity of 50 mPa s), the strand regime occurred within the peripheral speed range from 0.6 to 1.9 m s^{-1}.

The third hydrodynamic regime on the evaporating cylinder is indicated by the existence of the only one smooth and narrow peak on the RTD curve after passing through the multiple-peak area on increasing the wiper peripheral speed. In the event of sufficiently high wiper peripheral speed, the liquid is not able to form strands, as these strands are not stable, and a continuous downward-moving turbulent film is created on the evaporating area. A sharp and relatively narrow peak on the RTD curve indicates nonsignificant vertical mixing of the liquid in the film.

The shorter mean residence time in this turbulent regime, compared to the mean residence time in the strand regime, may also be related to the increased manifestation of a longitudinal wave (roulade) before the wiping element. At higher liquid loads, higher wiper peripheral speed, and higher viscosity, the liquid is not capable of entering the wiping element's passage channels, and part of it flows down at increased speed as a longitudinal wave before the wiping element. The liquid in the roulade rotates [11] and serves as a reservoir for replenishing the evaporated liquid in evaporator's lower parts. A wiping element design with a helical channel on its surface and with its rolling movement over the evaporating cylinder should restrict the longitudinal wave formation.

At low wiper peripheral speeds (Fig. 3, curve *1*), the RTD curve has the shape of a bell with an elongated tail as expected. At a higher speed (Fig. 3, curve *2*), the curve shape qualitatively changes. This indi-

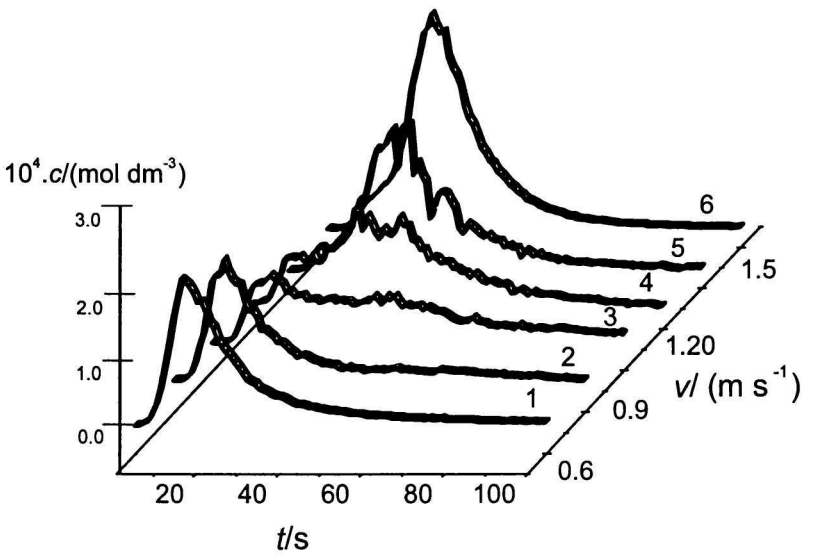

Fig. 3. Residence time distribution curves for liquid load of 4 dm^3 dm^{-1} h^{-1} and selected wiper peripheral speeds v. μ = 50 mPa s. *1.* v = 0.64 m s^{-1}, τ = 19.9 s; *2.* v = 0.92 m s^{-1}, τ = 25.1 s; *3.* v = 1.01 m s^{-1}, τ = 39.1 s; *4.* v = 1.21 m s^{-1}, τ = 34.8 s; *5.* v = 1.41 m s^{-1}, τ = 32.3 s; *6.* v = 1.63 m s^{-1}, τ = 30.1 s.

cates that the curve can be considered as a superimposition of a small number of elementary distribution curves the peaks of which are close to each other. This tendency is more markedly demonstrated on increasing the peripheral speed (Fig. 3, curve *3*) when the RTD curve is made up of a linear combination of a considerably higher number of elementary curves than in the previous case. When continuing to increase the peripheral speed (Fig. 3, curve *4*), the situation with augmented number of extremes indicates a similar multimodal case, but with a smaller half-width of the curves, *i.e.* the slopes of curves are steeper. Further peripheral speed increase leads to a decrease in the number of peaks (Fig. 3, curve *5*), but the differences between maxima and minima are becoming more distinct which can be related to disappearance of some elementary curves. This process continues with additional increase in peripheral speed, resulting in only one marked peak on the RTD curve (Fig. 3, curve *6*).

The downward transport of the liquid over the evaporating cylinder occurs during the strand regime in the form of thickened liquid strands, which are cut, formed and shifted downwards along the screw thread. The strands do not have enough time to disintegrate, being captured by the following row of wiping elements and forced to maintain the given shape. They leave the evaporator in a similar way. Therefore, it is possible to justify the idea that each such a strand is a carrier of the tracer, transporting it along the screw thread downwards if the tracer was present on the evaporator's top at the time of strand formation. This process is far from being ideal. Partial strand breaking followed by restoring occurs, while each strand has its own distribution curve. This approach enables us to deconvolute the resulting RTD curve into a series of elementary distribution curves so that the sums of conductivities of individual elementary curves create the contour of the summary RTD curve, while the sum of the areas below the elementary curves equals the area below the summary RTD curve, as required by the material balance equation.

The number and shape of the elementary distribution curves can be derived from the wiping element geometry, peripheral liquid load, and the duration of tracer feeding. At a liquid load of 4 $dm^3\ dm^{-1}\ h^{-1}$, the feed onto the evaporating cylinder of a 150-mm diameter is 5 $cm^3\ s^{-1}$. During the time of tracer injection into the feed of 0.5 s, the tracer mixes with 2.5 cm^3 of the liquid. According to Nusselt's equation for the film thickness

$$h = \sqrt[3]{\frac{3\mu\Gamma}{\rho^2 g}} \qquad (5)$$

the laminar film thickness formed by a liquid of 50 mPa s viscosity is 0.17 mm. The 2.5 cm^3 volume of the liquid covers a height of 3.12 cm. There are eight screws in the wiping element along this height, forming and directing the liquid into eight liquid strands. The tracer is then transported in these strands along the thread to the bottom of the evaporator according to the described model, more or less without perturbations. Because of irregularities in the strand formation,

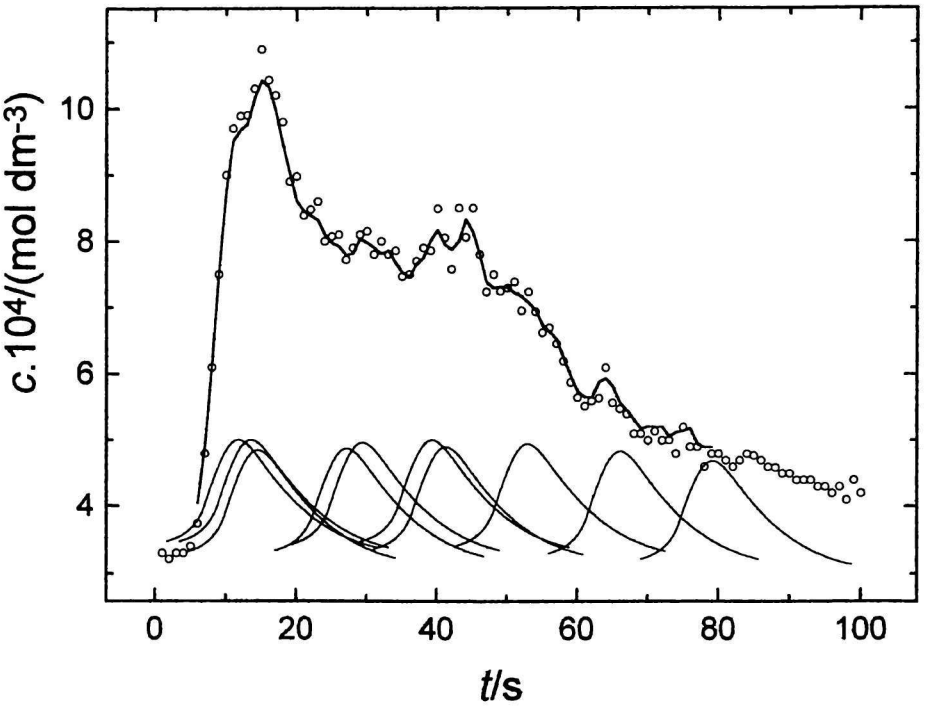

Fig. 4. Deconvolution of the RTD curve *3* from Fig. 3 (curve for $v = 1.01$ m s^{-1}) into elementary curves. The resulting curve represents superimposition of elementary curves. Statistical data: area = 0.00697 a.u., asymmetry factor $\rho = 2.0$.

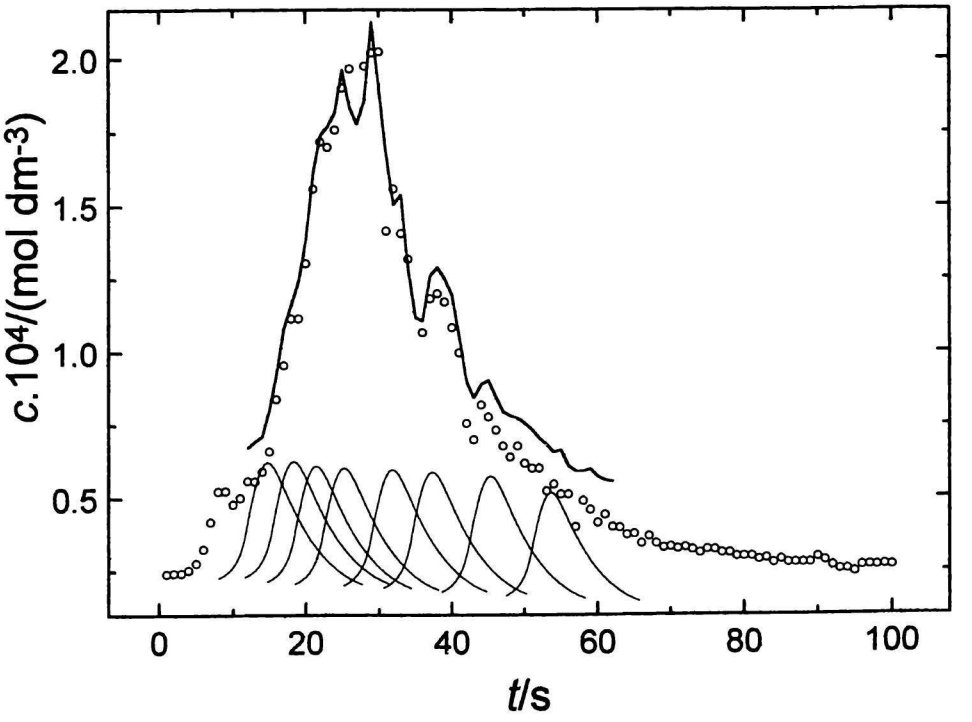

Fig. 5. Deconvolution of the RTD curve *5* from Fig. 3 (curve for $v = 1.41$ m s^{-1}) into elementary curves. The resulting curve represents superimposition of elementary curves. Statistical data: area = 0.00668 a.u., asymmetry factor $\rho = 1.9$.

a breakdown of the summary RTD curve into 8—12 elementary curves is justified. The area below a single elementary curve is then determined by the relevant portion of the total area. The elementary curve shape is determined in the same way to maintain the summary RTD curve contour. Higher and sharper peaks appearing at higher wiper peripheral speeds are related to a better filling of the thread channel on the wiper. On the contrary, some omitted peaks are manifested through deeper depressions on the summary RTD curve contour. Figs. 4 and 5 show deconvolution of the RTD curves *3* and *5* from Fig. 3 into elementary curves.

There exists a number of approximate functions for describing the bands. Individual types of approximate functions are characterized by various parameters, *e.g.* half-width of peak, maxima of the peak, asymmetry, *etc.* In the first attempt we tested the deconvolution of RTD curves using symmetrical gaussians, however statistical characteristics were not satisfied. Therefore an asymmetrical gaussian was used in the form

$$Y = Y_0 \exp\left\{-\left[\frac{(x - x_0)x_0}{x\Delta x}\right]^2\right\} \qquad (6)$$

This approximation seemed reasonable because the resulting RTD curve exhibits a certain degree of asymmetry. Both Y_0 and x_0 are considered as constants, Y_0 is the maximal intensity, x_0 is the position at which the gaussian reaches maximum intensity, and Δx is the half-width.

As mentioned above, in the case of our RTD curves it seemed reasonable to decompose curves on approximately 10 bands. Furthermore we have assumed that a physically relevant approximation will be to decompose RTD curve using one type of asymmetric gaussian, which follows the shape of the experimental curve and its parameters may be applied to $t \in (80, 100)$. Within these conditions we were able to decompose all curves for various speeds of wiper into their components with a good statistical characteristics (see Figs. 4 and 5).

In general, the strand regime of the liquid movement on the evaporator can be considered favourable from the point of view of molecular distillation. Heat transfer is a dynamic process depending on time, among other factors. During the prolonged optimum residence time of a liquid on the evaporating cylinder, an increased amount of heat, which is necessary to compensate for the enthalpy of evaporation, can be transferred into the liquid under more gentle conditions at a lower evaporating cylinder temperature [12]. Intensive mixing of the liquid on the evaporating cylinder helps compensate concentration and temperature gradients that are formed in the film as a result of intense evaporation.

The liquid dwells on the evaporating cylinder for a prolonged period of time, and there is enough liquid to be mixed during the increased hold-up on the evaporating cylinder. The mean residence time of the liquid continually grows, particularly in the curve *3* in Fig. 3, but it decreases with further peripheral speed

increase until it reaches steady state (approx. 30 s) which is considerably higher than in the previous one-peak RTD curve (30.1 s compared to 19.9 s).

Moreover, the wiper mixes the liquid maximally in the direction of the evaporator's axis in the strand regime, which enables enrichment with the more volatile component in the lower parts of the evaporator. This regime has the largest deviation from plug flow. Relatively long residence times indicate high wiping element's permeability for the liquid.

CONCLUSION

Measured distribution curves of the residence times of liquid on the evaporating cylinder during the strand regime show complex hydrodynamic conditions in the film wiped with profiled-surface roller wipers. The proposed physical model of the downward transport of the liquid on the evaporating cylinder in strands along the thread matches well with experimental values. From the viewpoint of molecular distillation, the strand regime is advantageous at increased retention of the liquid and increased residence time, because it enables the evaporator to reach high evaporation outputs at lower evaporator temperatures.

SYMBOLS

c	tracer concentration	mol dm^{-3}
g	gravity acceleration	m s^{-2}
h	film thickness	m
t	time	s
v	wiper peripheral speed	m s^{-1}
Γ	peripheral liquid load	dm^3 dm^{-1} h^{-1}
μ	dynamic viscosity	Pa s
τ	mean residence time	s
ρ	density	kg m^{-3}

REFERENCES

1. Watt, P. R., *Molecular Stills*, p. 182. Chapman & Hall, London, 1963.
2. Kukla, N., *Chem. Eng. World 32*, 33 (1997).
3. Cvengroš, J. and Tkáč, A., *Ind. Eng. Chem., Process Des. Dev. 17*, 246 (1978).
4. Lutišan, J. and Cvengroš, J., *Chem. Eng. J. 56*, 39 (1995).
5. Lutišan, J. and Cvengroš, J. *Sep. Sci. Technol. 30*, 3375 (1995).
6. Cvengroš, J. and Ďurčanský, J., *Slov.* 279 347 (1998).
7. Cvengroš, J., Pollák, Š., Micov, M., and Lutišan, J., *Chem. Eng. J.*, in press.
8. Cvengroš, J., Badin, V., and Pollák, Š., *Chem. Eng. J. 59*, 259 (1995).
9. Kirmse, D. W. and Westenberg, A. W. *Anal. Chem. 43*, 1035 (1971).
10. Kauppinen, J. K., Moffatt, D. J., Mantsch, H. H., and Cameron, D. G., *Appl. Spectrosc. 35*, 271 (1981).
11. Mutzenburg, A. B., *Chem. Eng. – Sept. 13*, 175 (1965).
12. Cvengroš, J., *Chem. Eng. Technol. 18*, 49 (1995).